Diverse Effects of β-Tubulin Mutations on Microtubule Formation and Function

Tim C. Huffaker, James H. Thomas, and David Botstein

Department of Biology, Massachusetts Institute of Technology, Cambridge, Massachusetts 02139

Abstract. We have used in vitro mutagenesis and gene replacement to construct five new cold-sensitive mutations in *TUB2*, the sole gene encoding β-tubulin in the yeast *Saccharomyces cerevisiae*. These and one previously isolated *tub2* mutant display diverse phenotypes that have allowed us to define the functions of yeast microtubules in vivo. At the restrictive temperature, all of the *tub2* mutations inhibit chromosome segregation and block the mitotic cell cycle. However, different microtubule arrays are present in these arrested cells depending on the *tub2* allele. One mutant (*tub2-401*) contains no detectable microtubules, two (*tub2-403* and *tub2-405*) contain greatly diminished levels of both nuclear and cytoplasmic microtubules, one (*tub2-104*) contains predominantly nuclear microtubules, one (*tub2-402*) contains predominantly cytoplasmic microtubules, and one (*tub2-404*) contains prominent nuclear and cytoplasmic microtubule arrays. Using these mutants we demonstrate here that cytoplasmic microtubules are necessary for nuclear migration during the mitotic cell cycle and for nuclear migration and fusion during conjugation; only those mutants that possess cytoplasmic microtubules are able to perform these functions. We also show that microtubules are not required for secretory vesicle transport in yeast; bud growth and invertase secretion occur in cells which contain no microtubules.

MICROTUBULES are found in an array of morphologically distinct structures in eukaryotes and have been implicated in a wide range of motile processes, including chromosome separation, intracellular transport of organelles, and maintenance of cell shape (reviewed in McIntosh, 1982; Roberts and Hyams, 1979). The precise mechanisms by which cells regulate the temporal and spatial assembly of microtubules, establish interactions between microtubules and other cell structures, and generate the force required for microtubule functions are not known. The key to understanding these processes is likely to reside in both the tubulin subunits that assemble to form microtubules and the nontubulin "associated" proteins that influence and mediate microtubule function. Much is known about the assembly properties of tubulin in vitro (reviewed in Dustin, 1984; Kirschner and Mitchison, 1986; McKiethan and Rosenbaum, 1984; Purich and Kristofferson, 1984) and several proteins have been identified which promote tubulin polymerization in vitro (reviewed in Olmsted, 1986). However, the relationship between these in vitro properties and the in vivo function of microtubules is largely uncertain. For this reason, we have chosen a genetic system that allows us to associate molecular characterizations with cellular functions.

The yeast *Saccharomyces cerevisiae* is a particularly tractable organism for such studies. It contains relatively simple microtubule arrays (Byers, 1981; Kilmartin and Adams, 1984; Peterson and Ris, 1976) that participate in a small number of well-defined and easily assayed events (Delgado and Conde, 1984; Pringle et al., 1986; Quinlan et al., 1980; Thomas et al., 1985). Its sophisticated genetic system and the small number of genes specifying each protein make mutants easy to find or construct. Yeast possesses a single gene that encodes β-tubulin, *TUB2* (Neff et al., 1983), and two genes that encode α-tubulins, *TUB1* and *TUB3* (Schatz et al., 1986). These proteins are highly conserved; >70% of the amino acid residues are identical between tubulins from yeast and animal cells. This high degree of sequence conservation suggests that the tubulin proteins from these cells have retained common biochemical properties. In support of this notion, it has been demonstrated that tubulin from yeast and animal cells will coassemble in vitro (Kilmartin, 1981; Pillus and Solomon, 1986). Significantly, a chimeric β-tubulin protein that contains both chicken and yeast sequences is incorporated efficiently into all of the microtubule structures of mouse fibroblasts in vivo (Bond et al., 1986).

This analysis of microtubules in yeast begins with the isolation of several cold-sensitive alleles of *TUB2*. Because β-tubulin must interact not only with other tubulins but also with nontubulin proteins that mediate specific microtubule functions, mutations in *TUB2* might produce different phenotypes. For example, a mutation that interferes with the formation of the α-tubulin–β-tubulin dimer will inhibit the

T. C. Huffaker's present address is Section of Biochemistry, Molecular and Cell Biology, Cornell University, Ithaca, NY 14853.

Table I. Yeast Strains Used in This Study

Strain	Genotype	Source
DBY947	*MATα ura3-52 ade2-101*	This laboratory
DBY1034	*MATa ura3-52 lys2-801 his4-539*	This laboratory
DBY1384	*MATa ura3-52 his4-539 tub2-104*	This laboratory
DBY1385	*MATα ura3-52 ade2-101 tub2-104*	This laboratory
DBY1571	*MATa lys2 leu2 hom3 can1-51*	This laboratory
DBY2022	*MATα ura3-52 ade2-101 tub2-401*	This study
DBY2023	*MATa ura3-52 lys2-801 his4-539 tub2-401*	This study
DBY2303	*MATα ura3-52 ade2-101 tub2-402*	This study
DBY2304	*MATa ura3-52 lys2-801 his4-539 tub2-402*	This study
DBY2305	*MATa ura3-52 lys2-801 his4-539 tub2-403*	This study
DBY2306	*MATα ura3-52 lys2-801 ade2-101 tub2-403*	This study
DBY2307	*MATα ura3-52 lys2-801 ade2-101 tub2-404*	This study
DBY2308	*MATa ura3-52 lys2-801 his4-539 tub2-404*	This study
DBY2309	*MATa ura3-52 lys2-801 his4-539 tub2-405*	This study
DBY2310	*MATα ura3-52 ade2-101 tub2-405*	This study
DBY4970	*MATα ura3-52 hom3 can1-51 tub2-104*	This study
DBY4971	*MATa leu2 hom3 can1-51 tub2-401*	This study
TH100	$\frac{MATa\ ura3\text{-}52\ his4\text{-}539\ +\ tub2\text{-}104}{MATα\ ura3\text{-}52\ +\ ade2\text{-}101\ +}$	DBY947 × DBY1384
TH101	$\frac{MATa\ ura3\text{-}52\ lys2\text{-}801\ his4\text{-}539\ +\ tub2\text{-}401}{MATα\ ura3\text{-}52\ +\ +\ ade2\text{-}101\ +}$	DBY947 × DBY2023
TH116	$\frac{MATa\ +\ lys2\ +\ leu2\ hom3\ can1\text{-}51}{MATα\ ura3\text{-}52\ +\ ade2\text{-}101\ +\ +\ +}$	DBY947 × DBY1571
TH117	$\frac{MATa\ +\ lys2\ +\ leu2\ hom3\ can1\text{-}51\ +}{MATα\ ura3\text{-}52\ +\ ade2\text{-}101\ +\ +\ +\ tub2\text{-}104}$	DBY1571 × DBY1385
TH118	$\frac{MATa\ ura3\text{-}52\ his4\text{-}539\ +\ +\ tub2\text{-}104}{MATα\ ura3\text{-}52\ +\ hom3\ can1\text{-}51\ tub2\text{-}104}$	DBY1384 × DBY4970
TH119	$\frac{MATa\ +\ lys2\ +\ leu2\ hom3\ can1\text{-}51\ +}{MATα\ ura3\text{-}52\ +\ ade2\text{-}101\ +\ +\ +\ tub2\text{-}401}$	DBY1571 × DBY2022
TH120	$\frac{MATa\ +\ +\ leu2\ hom3\ can1\text{-}51\ tub2\text{-}401}{MATα\ ura3\text{-}52\ ade2\text{-}101\ +\ +\ +\ tub2\text{-}401}$	DBY2022 × DBY4971
TH132	$\frac{MATa\ ura3\text{-}52\ lys2\text{-}801\ his4\text{-}539\ +}{MATα\ ura3\text{-}52\ +\ +\ ade2\text{-}101}$	DBY947 × DBY1034
TH133	$\frac{MATa\ ura3\text{-}52\ his4\text{-}539\ +\ tub2\text{-}104}{MATα\ ura3\text{-}52\ +\ ade2\text{-}101\ tub2\text{-}104}$	DBY1384 × DBY1385
TH134	$\frac{MATa\ ura3\text{-}52\ lys2\text{-}801\ his4\text{-}539\ +\ tub2\text{-}401}{MATα\ ura3\text{-}52\ +\ +\ ade2\text{-}101\ tub2\text{-}401}$	DBY2022 × DBY2023
TH135	$\frac{MATa\ ura3\text{-}52\ lys2\text{-}801\ his4\text{-}539\ +\ tub2\text{-}402}{MATα\ ura3\text{-}52\ +\ +\ ade2\text{-}101\ tub2\text{-}402}$	DBY2303 × DBY2304
TH136	$\frac{MATa\ ura3\text{-}52\ lys2\text{-}801\ his4\text{-}539\ +\ tub2\text{-}403}{MATα\ ura3\text{-}52\ lys2\text{-}801\ +\ ade2\text{-}101\ tub2\text{-}403}$	DBY2305 × DBY2306
TH137	$\frac{MATa\ ura3\text{-}52\ lys2\text{-}801\ his4\text{-}539\ +\ tub2\text{-}404}{MATα\ ura3\text{-}52\ lys2\text{-}801\ +\ ade2\text{-}101\ tub2\text{-}404}$	DBY2307 × DBY2308
TH138	$\frac{MATa\ ura3\text{-}52\ lys2\text{-}801\ his4\text{-}539\ +\ tub2\text{-}405}{MATα\ ura3\text{-}52\ +\ +\ ade2\text{-}101\ tub2\text{-}405}$	DBY2309 × DBY2310

All strains are essentially isogenic to S288C. The strains constructed for this study are the products of mutant isolations described in the text and standard crosses and tetrad analysis. Diploid strains are the products of matings between the indicated haploids.

assembly of all cellular microtubules and block all microtubule functions. On the other hand, a mutation that interferes only with the attachment of microtubules to the chromosomes will allow cytoplasmic microtubule function but block chromosome segregation. Thomas et al. (1985) showed that a single benomyl-resistant, cold-sensitive *tub2* mutation produces a cell cycle defect at mitosis. In this study, we characterize new mutations in *TUB2* that have diverse effects on microtubule formation and function in vivo. These mutations have allowed us to determine the roles of nuclear and cytoplasmic microtubules in yeast.

Materials and Methods

Strains and Media

Yeast strains used in this study are listed in Table I. *Escherichia coli* strain HB101* (DB1142) is *leu⁻ pro⁻ thr⁻ hsdR⁻ hsdM⁻ recA⁻*. DB6507 was also derived from HB101 and is *leu⁻ pro⁻ thr⁻ hsdR⁻ hsdM⁻ recA⁻ pyrF74*::Tn5.

Yeast media are essentially as described by Sherman et al. (1979). YEPD medium is 1% yeast extract, 2% Bacto-peptone, and 2% glucose. S medium[1] is 0.67% Yeast Nitrogen Base without amino acids: SD medium

1. *Abbreviations used in this paper*: DAPI, 4',6'-diamidino-2-phenylindole; S medium, 0.67% yeast Nitrogen Base without amino acids; SD medium, 0.67% Yeast Nitrogen Base without amino acids and 2% glucose.

also contains 2% glucose. S media was supplemented with 20 mg/liter uracil, 30 mg/liter lysine, 20 mg/liter histidine, 40 mg/liter adenine, 20 mg/liter methionine, and 200 mg/liter threonine as indicated. Canavanine, when added, was at 50 mg/liter. Solid media contained 2% agar.

Construction of Plasmids

The unique Sal I site of YIp5 (Scherer and Davis, 1979) was removed by cutting with Sal I, filling the 3′ ends with the Klenow fragment of DNA polymerase I (Rose and Botstein, 1983) and reclosing with DNA ligase. pRB428 (also called pJT71; Thomas, et al., 1985) contains the intact wild-type *TUB2* gene subcloned on a 3-kb Eco RI-Sph I fragment into the same sites on Sal I-filled YIp5.

pRB429 contains an incomplete copy of *TUB2* and was constructed as follows: pRB428 was cleaved partially with Eco RI and the 3′ ends were filled. This DNA was then cut to completion with Kpn I and the 7.1-kb Eco RI(filled)-Kpn I fragment was purified by agarose gel electrophoresis. pRB428 was also cut to completion with Xmn I and Kpn I and the 0.41-kb Xmn I-Kpn I fragment was isolated by PAGE. Ligation of the 7.1-kb Eco RI(filled)-Kpn I fragment to the 0.41-kb Xmn I-Kpn I fragment generated pRB429. Therefore, pRB429 contains an incomplete copy of *TUB2* that has one end in the fourth codon of *TUB2* and the other end 1.4 kb beyond the COOH-terminal coding sequence of *TUB2* in the Eco RI-Sph I backbone fragment of Sal I-filled YIp5.

Production of tub2 Mutants

The plasmid pRB429 was mutagenized in vitro. pRB429 was treated with DNase I to introduce a single random nick per plasmid (Shortle and Botstein, 1983). These nicks were converted to short gaps and the gaps were misrepaired by the nucleotide omission method of Shortle et al. (1982). The misrepair reactions and subsequent DNA isolations were done in eight separate pools: two pools each of minus dATP, minus dCTP, minus dGTP, and minus dTTP reactions.

The level of mutagenesis was checked by determining the percentage of plasmids that had lost *URA3* function as follows: DNA from each reaction was used to transform *E. coli* strain DB6507 selecting for ampicillin resistance. The frequency of Ura$^-$ mutations could be determined because DB6507 carries a *pyrF* mutation that is complemented by the wild-type yeast *URA3* gene. Uracil auxotrophs appeared in 1.6, 3.1, 3.4, and 4.4% of the cells transformed with DNA from the minus dATP, minus dCTP, minus dGTP, and minus dTTP reactions, respectively. Because the coding region of *URA3* is only ~10% of the plasmid sequence and not all mutations in *URA3* are expected to eliminate its activity, these data suggest that most of the plasmids were mutagenized by this protocol.

The eight pools of mutagenized DNA were used to transform eight separate cultures of the yeast strain DBY1034, selecting for uracil prototrophy on SD plates containing lysine and histidine at 26°C. Plasmid integration was directed to the chromosomal copy of *TUB2* by cutting the plasmid at the Kpn I site within the *TUB2* coding region before transformation. Homologous recombination occurs near the Kpn I site (Orr-Weaver et al., 1981) and produces a strain containing one intact and one disrupted copy of *TUB2* (see Fig. 1; Shortle et al., 1984). If the mutation on the plasmid lies between the Kpn I site and the 3′ end of the gene, the integrated mutation will lie in the intact copy of *TUB2* and even a recessive phenotype can be observed directly. If the mutation on the plasmid lies between the 5′ end of the gene and the Kpn I site, the integrated mutation will reside in the disrupted copy of *TUB2* and will not be detected. Thus, mutations recovered by this particular protocol should reside in the 3′ 70% of the *TUB2* coding region beyond the Kpn I site.

Approximately 17,000 transformants were replica plated to 26, 14, and 37°C plates. Colonies which grew at 26°C but failed to grow at either 14 or 37°C were picked and purified as single colonies. Eight colonies retested as cold sensitive; none retested as temperature sensitive. One of these mutants is cold sensitive for uracil prototrophy due, most likely, to mutation of the plasmid-borne *URA3* gene: it grows at 14°C on plates supplemented with uracil. Results of tetrad analysis show that five of the other seven cold-sensitive strains are cold-sensitive *tub2* mutants: these five cold-sensitive mutations are linked to the integrated plasmid sequences marked by *URA3*. The two cold-sensitive mutations that are not linked to *URA3* were not studied further. The *tub2-401*, *tub2-402*, and *tub2-403* alleles were generated by minus dATP reactions: *tub2-402* and *tub2-403* came from the same pool. The *tub2-404* and *tub2-405* alleles were generated by minus dCTP reactions but came from separate pools. Excision of plasmid sequences was selected by growing the primary transformants on 5-fluoro-orotic acid plates to select against *URA3* (Boeke et al., 1984).

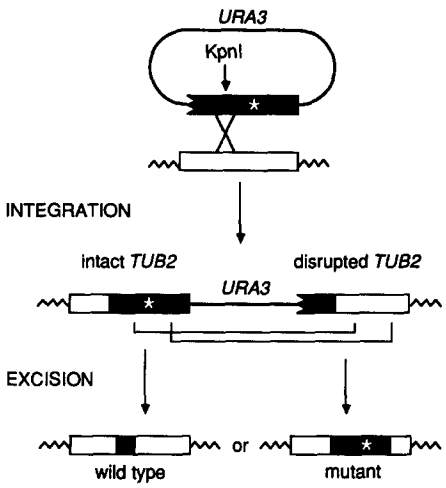

Figure 1. Construction of *tub2* mutants. The mutagenized plasmid (pRB429) contains a disrupted copy of *TUB2*; it is missing the first 14 nucleotides of coding sequence and all of the 5′ noncoding region of *TUB2*. It was mutagenized in vitro and cut with Kpn I before transformation to direct integration to the chromosomal *TUB2* locus. Integration results in a transformant bearing an intact and a disrupted *TUB2* gene flanking the *URA3*-selectable marker. In the example shown, the mutation (*) is located on the 3′ side of the Kpn I site in the plasmid and, thus, resides in the intact copy of *TUB2* in the transformant. Excision of the plasmid from this transformant can result in either a wild-type or mutant *tub2* strain. Solid bar represents *TUB2* sequences derived from plasmid; solid line represents flanking plasmid sequences; open bar represents *TUB2* sequences derived from chromosome; wavy line represents flanking chromosomal sequences.

Mapping and Sequencing the tub2 Mutations

pRB428 was used for fine structure mapping of the *tub2-401*, *tub2-402*, *tub2-403*, and *tub2-404* alleles. pRB429 was used for mapping the *tub2-405* allele. These plasmids contain unique Kpn I, Xho I, Bam HI, Hind III, and Sal I sites that lie within the *TUB2* gene. Digestions with pairs of these restriction enzymes generated the mapping plasmids illustrated in Fig. 2. The cut DNAs were phenol extracted and ethanol precipitated before transformation of yeast.

The method for the recovery of chromosomal *tub2* mutations on plasmids has been described (Thomas et al., 1985). Yeast DNA was prepared by the method of Holm et al. (1986).

DNA sequence analysis was performed as described by Sanger et al. (1977). The 350-bp Xho I-Bam HI fragment of the *tub2-401* and *tub2-402* alleles and the 280-bp Bam HI-Sal I fragment of the *tub2-403*, *tub2-404*, and *tub2-405* alleles were subcloned into the M13 vectors tg130 and tg131 (Amersham Corp., Arlington Heights, IL). For each allele the entire restriction fragment was sequenced on both strands.

Giemsa Staining of Yeast DNA

Cells were treated with Helly's fixative, immobilized on polylysine-coated multiwell slides, stained with Giemsa, and viewed using bright-field microscopy (Adams and Pringle, 1984; Robinow, 1975).

Measurement of the DNA Content of Yeast Cells

DNA was stained with propidium iodide using the protocol of Hutter and Eipel (1978). For each sample, the DNA content of 30,000 individual cells was determined by flow cytometry using a Cytofluorograph System 50H (Ortho Diagnostic Systems Inc., Westwood, MA).

Immunofluorescent Staining of Yeast Cells

Treatment of cells for immunofluorescence was essentially as described for formaldehyde fixation by Kilmartin and Adams (1984) except that the cell

walls were removed by incubation at 30°C for 30 min with 25 μg/ml Zymolyase 60,000 in 1.2 M sorbitol, 0.1 M potassium phosphate (pH 7.5), and 25 mM 2-mercaptoethanol. Rat monoclonal anti-yeast-α-tubulin antibody, YOL1/34, was a gift from J. Kilmartin (Medical Research Council Laboratory of Molecular Biology, Cambridge, United Kingdom). Rabbit polyclonal anti-yeast-β-tubulin antibody was a gift from F. Solomon (Massachusetts Institute of Technology, Cambridge, MA). Fluorescein-conjugated goat anti-rat IgG antiserum and fluorescein-conjugated goat anti-rabbit IgG antiserum were obtained from Cappel Laboratories (Malverne, PA). DNA was stained with 1 μg/ml 4',6'-diamidino-2-phenylindole (DAPI) for 5 min at room temperature before mounting.

Cells were viewed and photographed using a Zeiss Standard microscope equipped with epifluorescent and Nomarski optics and a Zeiss Plan-Neofluor 63× N.A. 1.25 objective. Hypersensitized Kodak Technical Pan 2415 film (Lumicon, Livermore, CA) was used for photography; it was developed with Kodak D-19 developer (Eastman Kodak Co., Rochester, NY).

Assays for Nuclear Fusion

Haploid cells were grown in supplemented SD medium at 26°C to no more than 5×10^6 cells/ml. 3×10^6 cells of each parent strain were mixed in liquid and filtered onto a sterile 25-mm HA millipore filter of pore size 0.45 μm (Dutcher and Hartwell, 1983). The filter was transferred to a fully supplemented SD plate, preequilibrated at the appropriate temperature, with the cells facing up. After 4 h at 26°C or 18 h at 11°C, the mated cells were washed from the filter with water, sonicated lightly to separate cells, and spread on a supplemented SD plate at 26°C. Large-budded zygotes were micromanipulated to predetermined positions and incubated at 26°C for 1–2 h to allow completion of cell division. First zygotic buds were then micromanipulated to another position and allowed to grow into colonies at 26°C. The colonies were tested for all relevant markers including mating type. In all experiments these colonies were either diploid or one of the parental haploid genotypes.

For immunofluorescence, cells were mated on filters at 11°C for 24 h, washed off the filters with 3.7% formaldehyde in 0.1 M potassium phosphate (pH 6.5), and prepared for immunofluorescence as described above.

Measurement of Invertase Activity

Cells were harvested by centrifugation, resuspended in 10 mM sodium azide, 10 mM potassium phosphate (pH 7.5), and kept on ice. External enzyme levels were measured using intact cells as described by Goldstein and Lampen (1975). Internal levels were measured in spheroplast lysates: cell walls were removed by incubation at 11°C for 1 h with 50 μg/ml Zymolyase 60,000 in 1.4 M sorbitol, 50 mM potassium phosphate (pH 7.5), and 25 mM 2-mercaptoethanol. Spheroplasts were pelleted and then lysed by addition of 1% Triton X-100. *N*-ethylmaleimide, 0.2 mM, was added to the enzyme assay to prevent interference by residual 2-mercaptoethanol (Novick and Schekman, 1979). To determine the total protein content of whole cells, we hydrolyzed them in 0.1 ml of 1 M potassium hydroxide at 100°C for 5 min and measured the protein in this hydrolysate by the method of Lowry et al. (1951).

Measurement of Chromosome Loss and Recombination

The assay for chromosome loss and recombination has been described by Wood (1982). Diploid strains, TH116–TH120, were grown in YEPD at 26°C. An aliquot was removed from each culture and the remainder was shifted to 11°C. After 12 and 24 h at 11°C, additional aliquots were removed from each culture. The cells in each aliquot were pelleted, washed, and resuspended in water, and sonicated lightly to separate cells. Appropriate volumes were plated on YEPD plates to measure the viable cells per ml and on SD plates containing uracil, methionine, threonine, and canavanine. After 7 d at 26°C (cells which have lost chromosomes grow slowly), the colonies were replica plated onto SD with uracil and canavanine and SD with uracil, methionine, threonine, and canavanine to determine the fraction of *can*^{R} colonies that are *hom3*. The ratio of *can*^{R} *HOM3*$^+$ cells per total viable cells is a measure of the frequency of recombination and the ratio of *can*^{R} *hom3* cells per total viable cells is a measure of the frequency of chromosome loss.

Measurement of Sporulation Efficiency

Sporulation of diploid strains (TH100, TH101, TH132, TH133, and TH134) was examined at the restrictive and permissive temperatures using the protocol of Simchen (1974). Presporulation and sporulation media were supplemented with uracil. Cells were incubated in sporulation medium for 2 h at 26°C before they were shifted to 11°C. This allowed most of the cells to complete their vegetative cycles at the permissive temperature. Sporulation was monitored by phase-contrast microscopy.

Results

Isolation of Cold-sensitive tub2 Mutants

Conditional-lethal alleles of *TUB2* were produced by in vitro mutagenesis of the *TUB2* gene and integration of the mutagenized gene into the yeast genome. Among 17,000 yeast transformants screened, five were shown to be cold-sensitive *tub2* mutants by four criteria. (*a*) All five fail to complement *tub2-104*, a previously isolated cold-sensitive mutation in *TUB2* (Thomas et al., 1985). *TUB2*$^+$*/tub2* diploids grow in the cold, while *tub2-104/tub2* diploids fail to grow in the cold. In addition, the new *tub2* alleles fail to complement each other. (*b*) In crosses to a *TUB2*$^+$ strain, each of these mutations is tightly linked to the integrated plasmid sequences that are marked by the *URA3* gene. In all tetrads, cold-sensitive spores are Ura$^+$ and cold-resistant spores are Ura$^-$. (*c*) When excision of the plasmid sequences is selected, both cold-sensitive and cold-resistant strains are produced. Excision may be considered as the reverse of the integration process, except that the site of recombination is not confined to the region near the Kpn I site. The mutation in a *tub2* allele may be removed from the genome with the plasmid sequences or left behind depending on the site of recombination (see Fig. 1). (*d*) All of the mutations are complemented by the cloned *TUB2* gene. Mutant haploids, transformed with a centromere-containing plasmid carrying the complete *TUB2* gene, grow in the cold.

The five new cold-sensitive *tub2* alleles are designated *tub2-401* through *tub2-405*. The remainder of this study uses strains from which the plasmid sequences have been excised leaving the mutation in the chromosome (see Fig. 1). This is the ideal construction because it regenerates the intact yeast chromosome which is altered only by the change(s) comprising the mutation.

DNA Sequence Analysis

The nucleotide sequence changes of the mutant alleles were determined by mapping each mutation in vivo to a segment of the *TUB2* gene and sequencing this segment of the cloned mutant gene. The mapping method has been previously described in detail (Shortle et al., 1984; Thomas et al., 1985). A mapping plasmid that contains the *TUB2* gene was cut at two restriction sites within *TUB2* and used to transform the cold-sensitive *tub2* strains. As with conventional deletion mapping, the absence of wild-type recombinants between a chromosomal mutation and a specific plasmid deletion localizes the mutation within that deletion interval. The results, shown in Fig. 2, indicate that the *tub2-401* and *tub2-402* mutations lie between the Xho I and Bam HI sites in *TUB2*, the *tub2-403* mutation lies between the Bam HI and Hind III sites, the *tub2-404* mutation lies between the Hind III and Sal I sites, and the *tub2-405* mutation lies between the Bam HI and Sal I sites.

The mutant *tub2* genes were recovered from the yeast chromosome onto recombinant plasmids. For each *tub2* allele, the entire region of the gene determined by mapping to contain the mutation was sequenced. The nucleotide changes

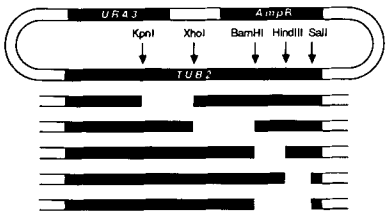

Number of Cs^+ Transformants / Total Tested				
tub2-401	*tub2-402*	*tub2-403*	*tub2-404*	*tub2-405*
3/61	10/62	11/30	13/30	23/71
0/62	0/62	7/30	14/30	31/83
8/30	11/30	0/62	11/30	nd
12/30	11/30	4/62	0/62	nd
nd	nd	nd	nd	0/75

Figure 2. Deletion mapping of *tub2* mutations by transformation with gapped linear plasmids. Each mapping plasmid was generated by cutting at the two restriction sites shown and used to transform each of the *tub2* mutant strains. In each case, many transformants were recovered; only those tested for marker rescue of the cold-sensitive phenotype are included in this figure. *nd*, not determined.

and the predicted amino acid changes comprising each mutation are shown in Fig. 3. Every base change in the five *tub2* alleles is consistent with the misincorporation reaction used (see Materials and Methods). Most of the mutations involve more than one change which agrees with the requirement that the entire gapped region must be filled. The *tub2-404* allele contains, in addition to two base substitutions, a deletion of nine nucleotides. This region of *TUB2* contains an eight-nucleotide direct repeat (see Fig. 3) and the deletion was most likely generated by strand slippage of the DNA near the gap site.

The *tub2-401* allele was generated in a reaction that omitted dATP and contains four base substitutions over a span of 38 nucleotides. Within this region are three A residues which are not altered. This type of incomplete base substitution with dATP omission was also seen by Shortle et al. (1982). These authors suggested that DNA polymerase must have incorporated an A residue either as dATP contaminating one of the other three dNTPs or as rATP which is present in the reaction as a cofactor for T4 DNA ligase.

Aside from the 3′ end bias mentioned above (see Materials and Methods), the mutations are distributed throughout the *TUB2* gene. Thus, there is no indication that mutations in a particular region of the *TUB2* gene are more likely to produce a cold-sensitive phenotype.

Cold Sensitivity and Benomyl Sensitivity

Although all of the *tub2* mutants were obtained by screening for failure to grow at 14°C, they differ in their degree of cold sensitivity. Growth of the *tub2-401* mutant is inhibited at temperatures as high as 20°C, while growth of the *tub2-402*, *tub2-404*, and *tub-405* mutants is completely blocked only at 11°C. The *tub2-403* mutant has an intermediate level of cold sensitivity, failing to grow at 16°C. None of the mutants are temperature sensitive: all grow well at 37°C.

Mutations in *TUB2* were obtained previously by selecting cells that are resistant to the microtubule-destabilizing drug benomyl (Thomas et al., 1985). To determine whether benomyl resistance is a phenotype common to all β-tubulin mutants, we tested the ability of the cold-sensitive *tub2* mutants to grow on various concentrations of benomyl at 26°C. The *tub2-402* allele does confer benomyl resistance, allowing cells to grow on 50 μg/ml benomyl, twice the concentration that inhibits wild-type growth. In contrast, the *tub2-403* and *tub2-405* mutants are supersensitive to benomyl, failing to grow on 5 μg/ml benomyl. The *tub2-401* and *tub2-404* mutants have an essentially wild-type sensitivity to benomyl. Thus, alterations in β-tubulin can result in either increased or decreased sensitivity to benomyl. There is no obvious correlation between the degree of cold sensitivity and benomyl sensitivity among these *tub2* mutants. Umesono et al. (1983) have made similar observations identifying mutations in the β-tubulin gene of the fission yeast *Schizosaccharomyces pombe* that produce altered drug sensitivities.

Mitotic Cell Cycle Arrest

Conditional-lethal mutations that block a specific stage of the cell cycle arrest asynchronously growing cells with a uniform terminal morphology at the nonpermissive temperature (Hartwell et al., 1973). Cells carrying the benomyl-resistant cold-sensitive *tub2* allele, *tub2-104*, exhibit such a uniform morphology after a shift to the restrictive temperature (Thomas et al., 1985). The same cell cycle arrest is observed for cells exposed to microtubule-destabilizing drugs (Pringle et al., 1986; Quinlan et al., 1980; Wood and Hartwell, 1982).

To determine whether the new *tub2* mutants exhibit a uniform arrest phenotype, we shifted asynchronous cultures to 11°C for 24 h (two generations). We have included the *tub2-104* mutant in this study. In all of the *tub2* mutant cultures, large-budded cells accumulated at the nonpermissive temperature (Fig. 4 *a*). The nuclear DNA in these cells was visualized by Giemsa staining. Most wild-type large-budded cells have completed chromosome separation and contain a DNA-staining region in both the mother and bud cell bodies. In contrast, almost all of the large bud-arrested mutant cells

```
tub2-401:                235                 240                 245
        ..val met ser gly val thr thr ser leu arg tyr pro gly gln leu..
        ..GTC ATG TCT GGT GTG ACA ACT TCA TTG CGT TAT CCC GGC CAA TTG..
              G                           G           G           T
              val                       ser         cys         leu

tub2-402:                   320
        ..phe phe arg gly lys..
        ..TTC TTT AGA GGT AAA..
                T G
                trp

tub2-403:                   375
        ..ser thr ser ile gln glu..
        ..TCC ACA TCT ATT CAA GAG..
              C G     G    GC
              pro     val arg

tub2-404:   420                 425                 430
        ..ser glu tyr gln gln tyr gln gln glu ala thr val..
        ..AGC GAA TAC CAA CAA TAC CAA GAG GCT ACT GTA..
              -- --- --- -                 G   G
            (     glu       )             gly ser

tub2-405:         390
        ..phe lys arg lys ala..
        ..TTC AAA AGA AAA GCT..
                C
                thr
```

Figure 3. Nucleotide and amino acid sequence changes of the *tub2* mutations. For each allele, only the region of *TUB2* that contains the mutation is shown. Numbering corresponds to the complete wild-type nucleotide and amino acid sequence. For each mutation, only the nucleotide change and the inferred amino acid alteration are shown. Dashed lines in the *tub2-404* sequence indicate that these nucleotides were deleted. The direct repeats in the wild-type sequence near the *tub2-404* mutation are underlined.

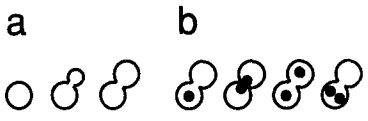

TUB2	41	39	20	22	3	75	0
tub2-104	2	3	95	87	5	2	6
tub2-401	4	8	88	94	0	2	4
tub2-402	14	24	62	81	9	8	2
tub2-403	10	15	75	86	2	11	1
tub2-404	15	27	58	89	4	5	2
tub2-405	9	7	84	84	9	6	1

Figure 4. Cell division cycle arrest. Diploid cells homozygous for the indicated *tub2* alleles (TH132 through TH138) were grown in SD containing uracil and lysine at 26°C, shifted to 11°C for 24 h, and stained with Giemsa. For each sample, 300 cells were counted. (*a*) The percentages of cells that were unbudded, small-budded, or large-budded are indicated. A large-budded cell possesses a bud whose diameter is at least three-fourths the diameter of the mother cell. All cultures contained 20–30% large-budded cells during growth at 26°C. (*b*) The percentages of large-budded cells that possessed a particular nuclear morphology are indicated. Four types of nuclear morphology were scored: an undivided nucleus in one cell body, an undivided nucleus in the bud neck, divided nuclei properly segregated into each cell body, and divided nuclei both located in one cell body.

contain a single staining region indicating that chromosome separation has not occurred (Fig. 4 *b*).

We used flow cytometry to measure the DNA contents of individual cells (Fig. 5). In wild-type cultures growing asynchronously at either 26 or 11°C, ~30% of the cells have not begun DNA replication (contain a G1 DNA content) and 55% of the cells have completed DNA replication (contain a G2 DNA content). The *tub2* mutant cultures grown at 26°C are similar to wild type: 20–30% of the cells contain a G1 DNA content and 50–60% of the cells contain a G2 DNA content. However, *tub2* mutant cultures that have been shifted to 11°C for 18 h contain almost exclusively cells with a G2 DNA content indicating that these mutations do not block DNA replication. Cultures of *tub2-104* or *tub2-401* cells, the mutants that give the tightest cell cycle arrest, contain no detectable cells with a G1 DNA content. As expected, cultures of the *tub2* mutants that do not give as tight a cell cycle arrest contain 5–10% cells with a G1 DNA content. In addition, some of the mutant cultures contain cells with twice the G2 DNA content. This suggests that a few of the cells (<5%) in these cultures undergo a second round of DNA replication.

Taken together, these results indicate that the *tub2* alleles do not inhibit DNA replication but all block chromosome segregation and completion of the cell cycle.

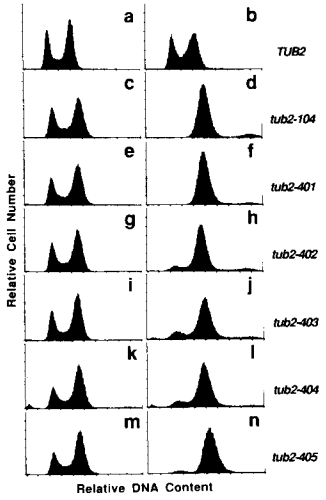

Figure 5. DNA content of cells. Diploid cells homozygous for the indicated *tub2* alleles (TH132–TH138) were grown in SD medium that contained uracil and lysine at 26°C and shifted to 11°C. (*a*, *c*, *e*, *g*, *i*, *k*, and *m*) Cells before shift to 11°C. (*b*, *d*, *f*, *h*, *j*, *l*, and *n*) Cells after shift to 11°C for 18 h. The DNA content of individual cells was determined by flow cytometry. (*a* and *b*) Wild type; (*c* and *d*) *tub2-104*; (*e* and *f*) *tub2-401*; (*g* and *h*) *tub2-402*; (*i* and *j*) *tub2-403*; (*k* and *l*) *tub2-404*; (*m* and *n*) *tub2-405*.

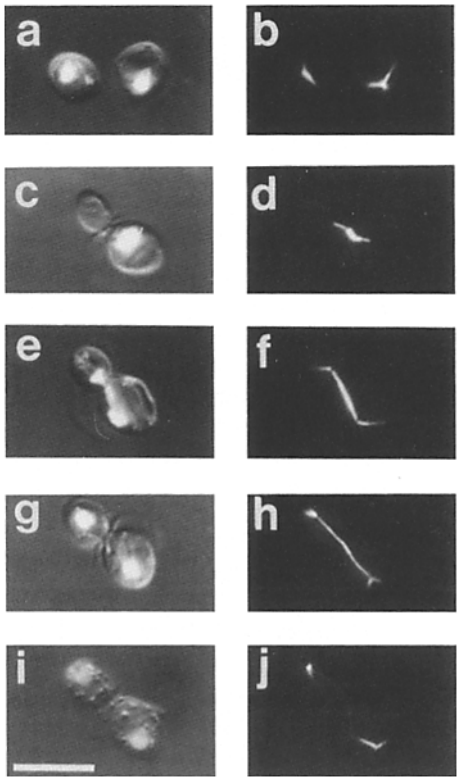

Figure 6. Fluorescence staining of wild-type cells. Wild-type diploid cells (TH132) were grown in SD medium that contained uracil and lysine at 26°C and shifted to 11°C for 24 h. (*a*, *c*, *e*, *g*, and *i*) Nomarski optics reveals cell morphology and DAPI fluorescence reveals cellular DNA. (*b*, *d*, *f*, *h*, and *j*) Immunofluorescence using α-tubulin–specific antibody reveals microtubules. Cells shown represent successive stages of the mitotic cell cycle. Bar, 10 μm.

Microtubule Assembly In Vivo

We have used indirect immunofluorescence with α-tubulin–specific antibody to visualize cellular microtubules in the *tub2* mutants. Fig. 6 shows microtubule staining of wild-type cells at successive stages of the mitotic cell cycle. Our results are similar to those obtained by Kilmartin and Adams (1984) which are in good agreement with previous electron microscopic observations of yeast microtubules (Byers, 1981; Peterson and Ris, 1976). The distribution of microtubules in wild-type cells grown at 26 or 11°C or in *tub2* mutant cells grown at 26°C are indistinguishable (not shown). However, after a shift to 11°C for 24 h, the patterns of microtubules in the large bud–arrested *tub2* mutant cells are strikingly different and specific for each *tub2* allele.

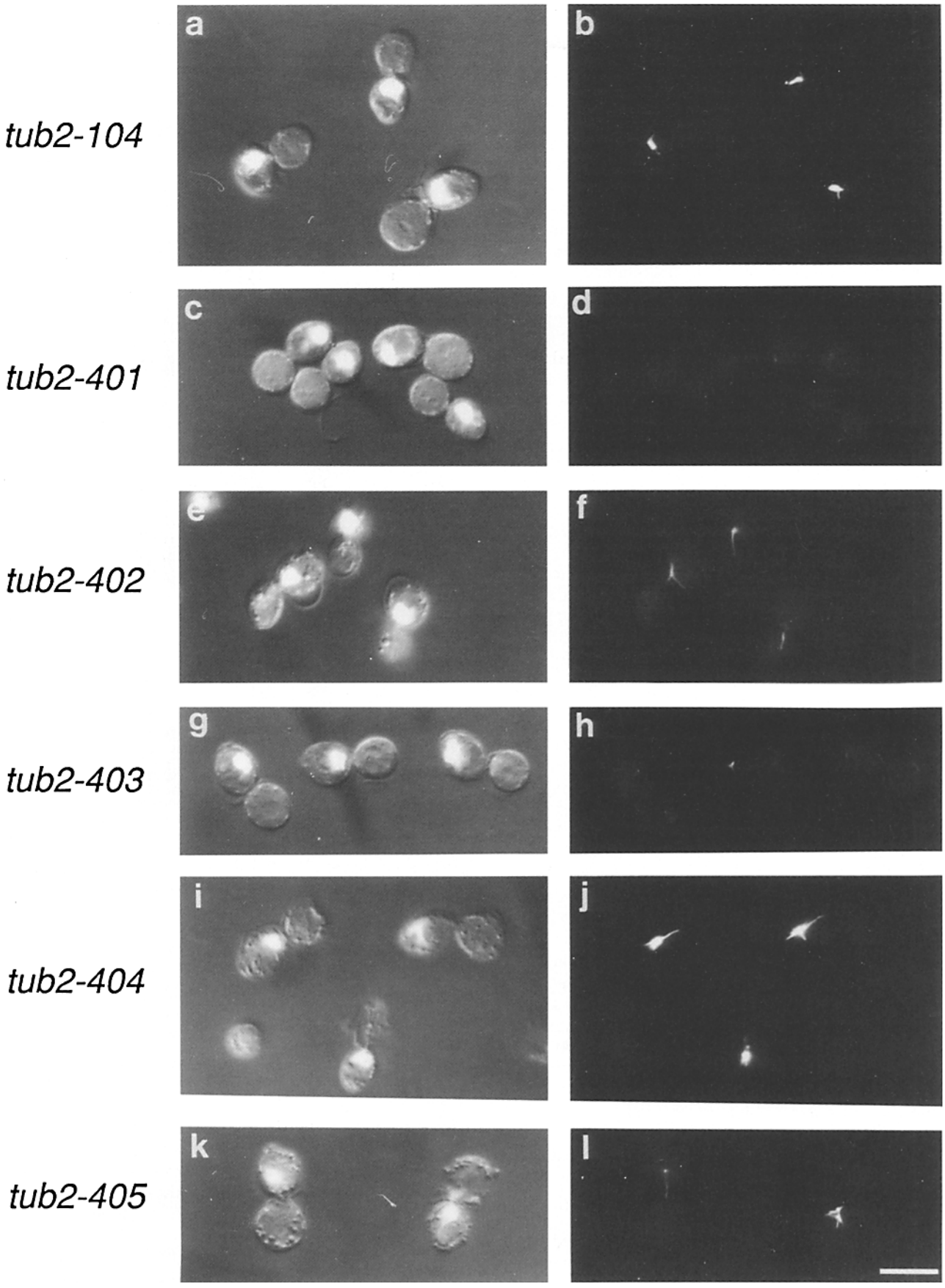

Figure 7. Fluorescence staining of *tub2* mutant cells. Diploid cells homozygous for the indicated *tub2* alleles (TH133–TH138) were grown in SD medium that contained uracil and lysine at 26°C and shifted to 11°C for 24 h. (*a*, *c*, *e*, *g*, *i*, and *k*) Nomarski optics reveals cell morphology and DAPI fluorescence reveals cellular DNA. (*b*, *d*, *f*, *h*, *j*, and *l*) Immunofluorescence using α-tubulin–specific antibody reveals microtubules. (*a* and *b*) *tub2-104*; (*c* and *d*) *tub2-401*; (*e* and *f*) *tub2-402*; (*g* and *h*) *tub2-403*; (*i* and *j*) *tub2-404*; (*k* and *l*) *tub2-405*. Bar, 10 μm.

Virtually no microtubules are observed in *tub2-401* cells (Fig. 7, *c* and *d*). Approximately 90% of the cells have no staining. The other 10% contain one or two faint dots coincident with the nuclear staining that probably correspond to the spindle pole bodies. Microtubule fibers disappear in <1 h after shifting to 11°C but most cells retain the dots for several hours. This result could be due to loss of microtubules in the cold or to an alteration in the microtubules that blocks their binding site for the antibody. To examine this latter possibility, we used another antibody that recognizes specifically the COOH-terminal 12-amino acid peptide of yeast β-tubulin, a region of β-tubulin not altered by the *tub2-401* mutation. This antibody also fails to detect any microtubule structures in this mutant (not shown), confirming that the *tub2-401* mutant does not contain microtubules in the cold.

The *tub2-403*- (Fig. 7, *g* and *h*) and *tub2-405*- (Fig. 7, *k* and *l*) arrested cells both contain greatly diminished levels of microtubules. In *tub2-403* cells, ~60% have no staining, 10% contain dots, and 30% contain very short faint fibers. In *tub2-405* cells, ~10% have no staining, 20% contain dots, and 70% contain faint fibers. The fibers in *tub2-405* cells are usually longer and brighter than those in *tub2-403* cells. The dots and fibers are always located in the region of the cell that contains the nucleus and presumably represent nuclear or cytoplasmic microtubules extending from the spindle pole bodies.

Virtually all of the *tub2-104*- (Fig. 7, *a* and *b*) arrested cells contain brightly staining nuclear microtubules that appear similar to the short mitotic spindle found in wild-type cells (see Fig. 6 *d*). In ~75% of these cells, extremely short cytoplasmic microtubules can be observed extending from the ends of the spindle; no cytoplasmic microtubules are detected in the other 25% of the cells.

Most *tub2-402*- (Fig. 7, *e* and *f*) arrested cells (60–70%) contain long microtubules extending from one or two bright dots near the edge of the nuclear staining. While some of these microtubules could be nuclear, the majority clearly diverge from the nuclear staining region and are most likely cytoplasmic. None of these cells contain the brightly staining spindle structure that is found in wild-type cells. The other 30–40% of the cells contain only dots of staining.

The *tub2-404*- (Fig. 7, *i* and *j*) arrested cells contain both brightly staining spindle microtubules and prominent cytoplasmic microtubules. These microtubule arrays are similar to the arrays observed in wild-type cells before spindle elongation (see Fig. 6 *d*). However, the intensity of staining and the length of the cytoplasmic microtubules is often greater in the *tub2-404* cells, indicating that excess microtubules are present. The intense staining at both spindle and cytoplasmic microtubules is found in 75% of the arrested cells; the other cells contain diminished staining and incomplete spindles.

Based on their degrees of microtubule assembly, the *tub2* mutants represent several different phenotypic classes. The *tub2-401* mutation appears to be a totally nonfunctional allele causing the loss of all detectable microtubules in the cold. This is the most extreme possible conditional-lethal mutation; however, it should be emphasized that this is not a null mutation in the sense of a deletion. The *tub2-403* and *tub2-405* mutations are also defective alleles that affect both nuclear and cytoplasmic microtubules; the *tub2-403* mutation causes a more severe defect than the *tub2-405* mutation. The *tub2-104* and *tub2-402* mutations affect specific classes of microtubules. The *tub2-104* mutation affects mainly the presence of cytoplasmic microtubules while the *tub2-402* mutation affects mainly the presence of the spindle microtubules. The *tub2-404* mutation allows the production of both classes of microtubules but prevents spindle elongation.

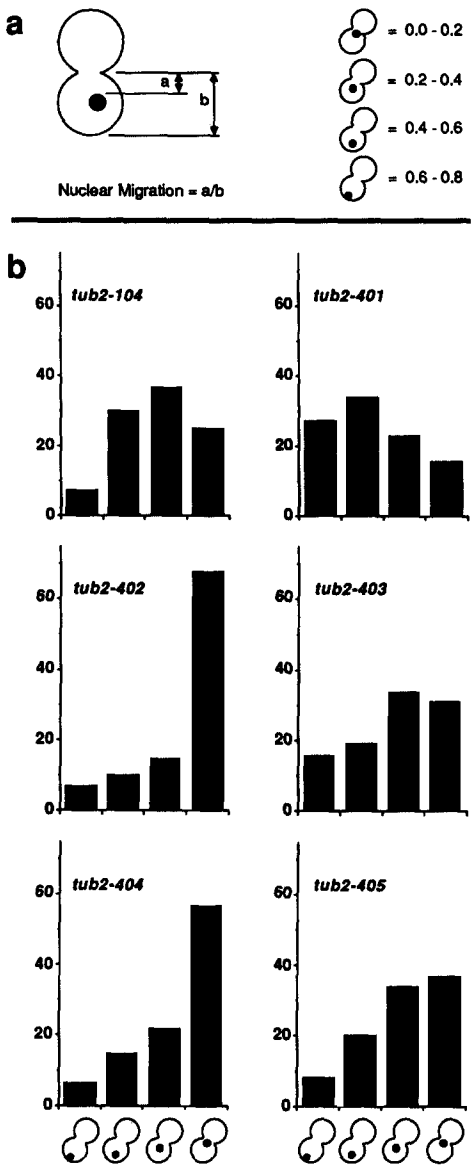

Figure 8. Measurement of nuclear migration. Diploid cells homozygous for the indicated *tub2* alleles (TH133–TH138) were grown in SD medium that contained uracil and lysine at 26°C, shifted to 11°C for 24 h, and stained with Giemsa. (*a*) Nuclear migration was quantitated by calculating the ratio of the shortest distance from the bud neck to any point on the nucleus and the maximum length of the mother cell as measured from the bud neck. (*b*) Graphs show the percentages of *tub2* cells with nuclei within each of four nuclear position intervals. For each sample, the position of the nucleus in 100–200 individual cells was calculated.

Nuclear Migration during the Mitotic Cell Cycle

Shortly after the initiation of bud formation, the nucleus migrates to the bud neck (Pringle and Hartwell, 1981). This nuclear position is necessary to ensure that the subsequent nu-

clear division delivers one set of chromosomes to each daughter cell. The observation that cytoplasmic microtubules are attached to the nuclear envelope through the spindle pole body and precede the nucleus into the bud neck led to the suggestion that they play a role in nuclear migration (Adams and Pringle, 1984). This idea was substantiated by the observation that microtubule-destabilizing drugs inhibit nuclear migration in yeast (Pringle et al., 1986; Wood and Hartwell, 1982). Therefore we examined the effects of the *tub2* mutations on proper nuclear migration.

Wild-type and *tub2* mutant cells were shifted to 11°C for 24 h and stained with Giemsa. Nuclear migration was quantitated by measuring the position of the nucleus in individual cells (see Fig. 8 *a*). In wild-type cells with any visible bud, undivided nuclei tend to be close to the bud neck; 76% of the undivided nuclei were located near the bud neck (nuclear migration <0.2). As described above, *tub2* mutants arrest as predominantly large-budded cells containing a single nucleus that has not elongated through the bud neck. The nuclear migration ratio was determined for these cells only and the results are shown in Fig. 8 *b*.

In cells carrying the extreme nonfunctional allele, *tub2-401*, nuclear migration to the bud neck is blocked; only 16% of the nuclei are located near the bud neck. In cells carrying the partially functional alleles, *tub2-403* and *tub2-405*, most nuclear migration is blocked; 31 and 37%, respectively, of the nuclei are near the bud neck. The *tub2-104* allele that affects primarily cytoplasmic microtubule formation also blocks nuclear migration; only 25% of the cells have nuclei near the bud neck. In contrast, the *tub2-402* and *tub2-404* alleles that do not inhibit cytoplasmic microtubule formation have very little effect on nuclear migration; 68 and 57%, respectively, of the nuclei in these cells are located near the bud neck.

These results show a correlation between the presence of cytoplasmic microtubules and the ability of cells to transport nuclei to the bud necks. Significantly, nuclear migration occurs in *tub2-402* mutants even though most of these cells contain exclusively cytoplasmic microtubules. Thus, the *tub2* mutants indicate that cytoplasmic microtubules, but not nuclear microtubules, are necessary for nuclear migration in yeast.

Nuclear Fusion during Conjugation

Diploid cells are formed from two haploids of opposite mating type by conjugation. Conjugation involves cytoplasmic and nuclear fusion and produces a zygote with a single diploid nucleus. Cytoplasmic microtubules appear to interconnect the spindle pole bodies of the two haploid nuclei before fusion and nuclear fusion is initiated at the spindle pole bodies (Byers, 1981; Byers and Goetsch, 1975). This arrangement of microtubule fibers during conjugation suggests that they play a role in nuclear fusion by moving the nuclei together. In support of this model, benomyl treatment (Delgado and Conde, 1984) and a mutation that produces aberrant extranuclear microtubules (Rose and Fink, 1987) have been shown to reduce the frequency of nuclear fusion.

A genetic test for nuclear fusion is based on the observation by Conde and Fink (1976) that zygotes that fail in nuclear fusion transfer one of the parental haploid nuclei into the first zygotic bud. Thus, when nuclear fusion fails, the first zygotic bud produces a haploid rather than a diploid cell. To test the effect of the *tub2* mutations on nuclear fusion, we analyzed the first zygotic buds produced by mating two *tub2* mutants. The results of several crosses are shown in Table II. As expected, *TUB2*$^+$ × *TUB2*$^+$ crosses at 26 or 11°C and *tub2* × *tub2* mutant crosses at 26°C produced mainly diploid first zygotic buds. However, when a *tub2* × *tub2* mutant cross was performed at 11°C with *tub2-104*, *tub2-401*, *tub2-403*, or *tub2-405* alleles, all of which affect cytoplasmic microtubules to some extent, most of the first zygotic buds were haploids. However, the *tub2-402* and *tub2-404* alleles, which allow the formation of cytoplasmic microtubules, again behaved differently. Crosses with these alleles at 11°C produced 60 and 83% diploids, respectively. As was the case with nuclear migration during the mitotic cell cycle, these results indicate that cytoplasmic microtubules are necessary for nuclear fusion during conjugation. Two additional crosses, *TUB2*$^+$ × *tub2-104* and *TUB2*$^+$ × *tub2-401*, produced almost all diploids at 11°C. This indicates that only one parent cell needs to produce wild-type β-tubulin to allow proper nuclear fusion.

Table II. Genetic Analysis of Nuclear Fusion

	Diploids/total			
	26°C*		11°C	
TUB2 × *TUB2*	19/19	(100%)	8/8	(100%)
tub2-104 × *tub2-104*	21/22	(95%)	2/20	(10%)
tub2-401 × *tub2-401*	14/14	(100%)	0/15	(0%)
tub2-402 × *tub2-402*	30/30	(100%)	32/53	(60%)
tub2-403 × *tub2-403*	36/36	(100%)	4/26	(15%)
tub2-404 × *tub2-404*	18/18	(100%)	39/47	(83%)
tub2-405 × *tub2-405*	19/19	(100%)	0/17	(0%)
TUB2 × *tub2-104*	23/24	(96%)	22/23	(96%)
TUB2 × *tub2-401*	20/20	(100%)	22/22	(100%)

* 26°C and 11°C refer to the temperature at which matings were performed.

These genetic results were confirmed by fluorescent microscopic observation of zygotes formed at 11°C. Fig. 9 shows nuclear and microtubule staining of wild-type zygotes at various stages after mating. A newly formed zygote contains nuclei that are located near each other and appear to be connected by microtubules (Fig. 9, *a* and *b*). Shortly after nuclear fusion, the zygote enters the mitotic cycle. A bud develops at the cell surface and a short mitotic spindle forms across the diploid nucleus (Fig. 9, *c* and *d*). Spindle elongation segregates the chromosomes between the zygote and bud (Fig. 9, *e* and *f*).

Fig. 9 also shows staining of large-budded zygotes formed by mating *tub2* mutant haploids at 11°C. Because the *tub2* mutations block nuclear division, nuclei are not observed in the first zygotic buds. Zygotes formed by mating *tub2-104*, *tub2-401*, *tub2-403*, or *tub2-405* haploids contain two separate nuclear staining regions (Fig. 9, *g*, *i*, *m*, and *q*) indicating that movement of the nuclei toward each other has not occurred. In contrast, the *tub2-404* zygotes contain a single nuclear staining region (Fig. 9, *o*) indicating that nuclear movement and fusion have occurred. Zygotes formed by mating *tub2-402* haploids are of both types: approximately half contain two nuclear staining regions and half contain a single nuclear staining region (Fig. 9 *k*). The microtubule

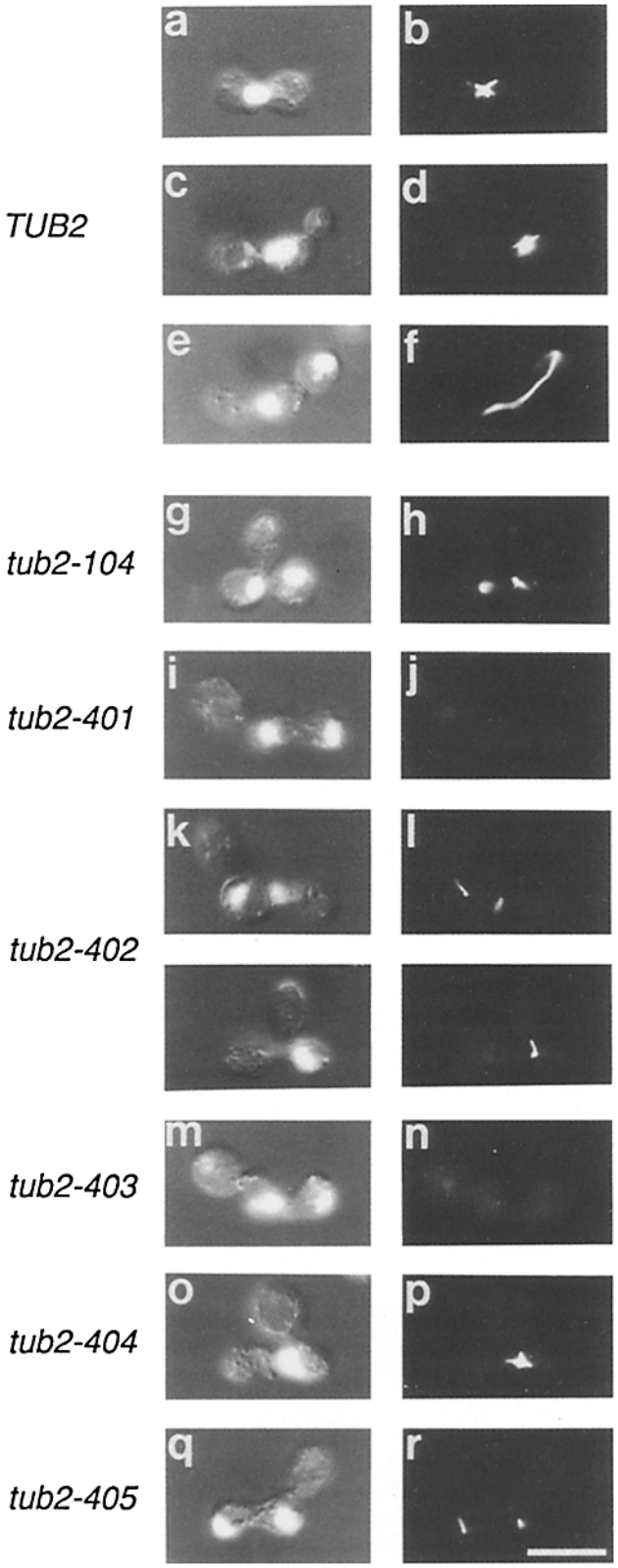

Figure 9. Fluorescence staining of zygotes. Zygotes were formed by mating wild-type and *tub2* mutant cells at 11°C as described in Materials and Methods. (*a*, *c*, *e*, *g*, *i*, *k*, *m*, *o*, and *q*) Nomarski optics reveals cell morphology and DAPI fluorescence reveals cellular DNA. (*b*, *d*, *f*, *h*, *j*, *l*, *n*, *p*, and *r*) Immunofluorescence using α-tubulin-specific antibody reveals microtubules. (*a–f*) Wild-type cells (DBY947 × DBY1034) at successive stages of conjugation; (*g* and *h*) *tub2-104* (DBY1384 × DBY1385); (*i* and *j*) *tub2-401* (DBY2022 × DBY2023); (*k* and *l*) *tub2-402* (DBY2303 × DBY2304); (*m* and *n*) *tub2-403* (DBY2305 × DBY2306); (*o* and *p*) *tub2-404* (DBY2307 × DBY2308); (*q* and *r*) *tub2-405* (DBY2309 × DBY2310). Bar, 10 μm.

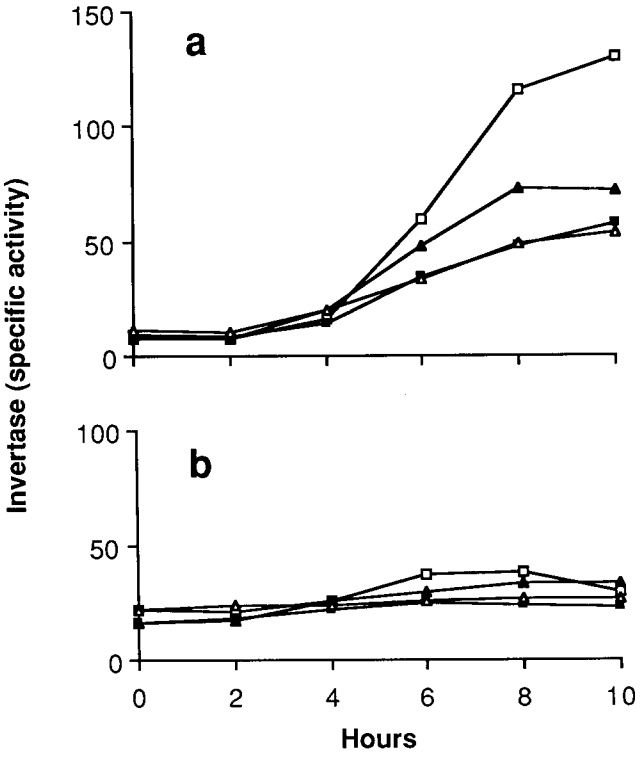

Figure 10. Secretion of invertase. Haploid cells were grown in supplemented S medium containing 5% glucose at 26°C. At $t = 0$ cells were pelleted, resuspended in supplemented S medium containing 0.1% glucose, and incubated at 11°C. At 2-h intervals, aliquots were removed and assayed for external and internal pools of invertase. (*a*) External levels. (*b*) Internal levels. (□) Wild-type (DBY1034); (▲) *tub2-104* (DBY1384); (■) *tub2-401* (DBY2023); (△) *tub2-403* (DBY2305).

structures observed in mutant zygotes are similar to those seen in the corresponding mutants after arrest of mitotic growth.

Invertase Secretion

During the budded portion of the cell cycle, surface growth and protein secretion are primarily restricted to the bud (Field and Schekman, 1980; Tkacz and Lampen, 1972, 1973) and are mediated by membrane-bounded organelles (Novick and Schekman, 1979). Cytoplasmic microtubules extend into the bud and lie close to these secretory vesicles (Byers, 1981; Byers and Goetsch, 1975; Kilmartin and Adams, 1984). This observation led to the suggestion that microtubules play a role in bud formation by transporting secretory vesicles into the growing bud. Clearly, the arrest of the *tub2* mutants as large-budded cells indicates that microtubules are not required for cell surface growth.

To address more directly the involvement of microtubules in the transport of secretory vesicles, we tested the effects of

tub2 mutations on the secretion of a specific periplasmic protein. Invertase is the product of the *SUC2* gene (Carlson and Botstein, 1982). This gene encodes two transcripts, a constitutively synthesized transcript whose product remains in the cytoplasm and a hexose-repressed transcript whose product is secreted into the periplasm. Secretion of invertase was followed in wild-type cells and three of the *tub2* mutants: *tub2-104*, *tub2-401*, and *tub2-403*. Cultures were grown at 26°C in repressing medium and then the cells were shifted into derepressing medium at 11°C to observe the ability of cells to secrete newly synthesized invertase in the cold. The external pool of enzyme in the wild-type culture began to rise 2 h after the shift, continued to increase over the next 6 h, and then leveled off (Fig. 10 *a*). The secretion of invertase in *tub2* mutant cultures followed the same kinetics except that the external pool leveled off at ~50% of the wild-type amount. This difference could be due to either a partial secretion defect or a decrease in the total amount of invertase synthesized in the mutants. These two possibilities were distinguished by measuring the levels of invertase inside the cells. If the mutants synthesized wild-type levels of invertase but secreted only half, the remainder would accumulate inside the cells. Many temperature-sensitive secretion mutants accumulate large pools of intracellular invertase (Novick et al., 1980) and it is unlikely that a *tub2* mutation would cause invertase to be unstable in the cell. There was no accumulation of enzyme inside the cells in any of the *tub2* cultures during the course of the experiment (Fig. 10 *b*) indicating that secretion of invertase is not blocked in these mutants.

Chromosome Loss and Mitotic Recombination

We have shown by cytological studies that chromosome segregation is blocked by the *tub2* mutations. A functional assay of chromosome segregation efficiency is based on the measurement of chromosome loss. The fidelity of mitotic chromosome segregation in *S. cerevisiae* is high: nondisjunction events occur at a frequency per chromosome of <1 in 10^5 cell divisions (Hartwell and Smith, 1985). Impairment of tubulin activity by drug treatment dramatically increases this rate (Wood, 1982). Therefore, our expectation was that the *tub2* mutants would exhibit an increase in chromosome loss after incubation at the restrictive temperature.

The frequency of loss of chromosome V was tested using the method described by Wood (1982). Chromosome loss in *tub2-104/tub2-104* diploids grown at 26°C was not significantly greater than in wild-type diploids (Table III). However, after incubation at 11°C for 24 h, chromosome loss in these diploids was ~40-fold greater than the wild-type rate. In *tub2-401/tub2-401* diploids grown at 26°C, chromosome loss was ~50 times the wild-type rate. When these cells were shifted to 11°C for 24 h, the frequency of chromosome loss increased to ~200 times the wild-type rate. While both of the *tub2* mutants tested showed increased rates of chromosome loss, the extent of the defect is clearly allele specific.

Hartwell and Smith (1985) observed that most of the *cdc* mutants that are defective in the nuclear division pathway of the cell cycle show increased rates of chromosome loss. However, many of these mutations elevate the frequency of mitotic recombination as well. For this class of mutants, the elevated chromosome loss frequencies are probably not due to nondisjunction but to defects in DNA metabolism. A defect in DNA metabolism may leave lesions in the DNA that promote increases in both mitotic recombination and chromosome loss. As expected for mutations that affect only chromosome segregation, the *tub2* alleles did not have any significant effect on mitotic recombination (Table III).

Table III. Chromosome Loss and Recombination

	Frequency ($\times 10^5$)					
	Recombination			Chromosome loss		
	0 h*	12 h	24 h	0 h	12 h	24 h
TUB2/TUB2	27	26	26	1.1	1.6	1.0
tub2-104/tub2-104	16	22	27	2.6	3.8	41.0
tub2-401/tub2-401	27	29	40	48	110	220
TUB2/tub2-104	16	nd	26	0.8	ND	3.9
TUB2/tub2-401	17	nd	28	7.8	ND	20.0

* Time cells were incubated at 11°C.

Meiosis and Sporulation

Yeast is induced to undergo sporulation by starvation for a variety of nutrients. Sporulation in yeast involves a classical meiosis, including reductional and equational chromosome segregations (Esposito and Klapholtz, 1981). These chromosome segregation events are assumed to be mediated by microtubules. Typically, the sporulating parent is diploid, giving rise to haploid genomes that are packaged into four individual spore walls to produce a tetrad.

We tested whether the product of the *TUB2* gene is required for meiosis by determining the effect of two of the *tub2* mutations on sporulation. With wild-type diploids, 75% of the cells produced tetrads at 26°C and 55% produced tetrads at 11°C. Maximum sporulation was achieved in 2 d at 26°C and 7 d at 11°C. Homozygous *tub2-104* and *tub2-401* diploids sporulated well at 26°C (59 and 68% tetrads, respectively) but failed to sporulate at 11°C. Among 500 cells examined for each mutant, no tetrads, triads, or dyads were observed. As in mitosis, the *tub2* mutations are recessive in meiosis: *TUB2*$^+$*/tub2-104* and *TUB2*$^+$*/tub2-401* diploids sporulated with the same efficiency as *TUB2*$^+$*/TUB2*$^+$ diploids at both 26 and 11°C.

Discussion

In this study we describe the construction and isolation of five cold-sensitive mutations in *TUB2*, the sole gene that encodes β-tubulin in *Saccharomyces cerevisiae.* Phenotypic analysis of these and one previously obtained cold-sensitive *tub2* mutation has shown that mutations in *TUB2* can have diverse effects on microtubule formation and function in vivo. We have used these mutations to determine the roles of nuclear and cytoplasmic microtubules in yeast. As predicted from cytological (Adams and Pringle, 1984; Byers, 1981; Byers and Goetsch, 1975) and drug studies (Delgado and Conde, 1984; Pringle et al., 1986; Quinlan et al., 1980; Wood and Hartwell, 1982), nuclear microtubules are required for chromosome segregation, and cytoplasmic microtubules are required for nuclear migration during the mitotic cell cycle and nuclear fusion during conjugation. Contrary to previous suggestions (Byers, 1981; Byers and Goetsch, 1975), cytoplasmic microtubules do not appear to play a role in the transport of secretory vesicles to the bud.

All of the tub2 Mutations Block Chromosome Segregation

When strains carrying a cold-sensitive *tub2* mutation are shifted to the nonpermissive temperature, they arrest mitotic growth at a specific stage of the cell cycle and accumulate as large-budded cells containing a single undivided nucleus. The cells arrest after DNA replication indicating that the block in nuclear division is due to a failure of chromosome segregation. As expected for mutations that interfere with chromosome segregation, both of the *tub2* alleles tested increased the rates of chromosome loss after incubation at the restrictive temperature.

While the cell cycle arrest is similar for all six of the *tub2* mutants, the microtubule structures observed in these arrested cells vary depending on the mutant allele. This suggests that the specific cause of the nuclear division block is not the same for all of the mutants. Very few, if any, of the *tub2-401-*, *tub2-402-*, *tub2-403-*, and *tub2-405*-arrested cells contain nuclear microtubules indicating that the defect in chromosome segregation in these mutants is due to a failure to construct a mitotic spindle. On the other hand, the *tub2-404*–arrested cells do contain spindle microtubules. The defect in this mutant is not simply an inability to assemble microtubules, but may involve either a specific problem in spindle formation that can not be detected by immunofluorescence or a defect in spindle function once it is assembled.

We are unable to determine whether cytoplasmic microtubule function is needed for nuclear division. The *tub2-104*–arrested cells contain nuclear but lack most cytoplasmic microtubules. In this case the nuclear division block could be due to a defect in spindle function or be related to a lack of cytoplasmic microtubule function. Cytoplasmic microtubules could play a direct role in nuclear division or be required to perform a function that is a prerequisite for nuclear division. We have shown that cytoplasmic microtubules are necessary for migration of the nucleus to the bud neck, but it is unlikely that nuclear division per se depends on this process: the *cdc24* mutant undergoes several rounds of nuclear division in the absence of bud formation, indicating that at least under some circumstances nuclear division can occur without migration into a bud neck (Pringle and Hartwell, 1981). If cytoplasmic microtubules do not play a role in nuclear division, we would expect mutants defective only in cytoplasmic microtubule function to undergo nuclear division in the absence of nuclear migration. This event would produce a binucleate mother cell. While we have not isolated a *tub2* mutant with this exact phenotype, a small percentage of the *tub2-104*–arrested cells do contain two nuclear staining regions in one of the cell bodies (see Fig. 4).

Cytoplasmic Microtubules Are Essential for Nuclear Migration during the Mitotic Cell Cycle

Nuclear migration to the bud neck during the mitotic cell cycle is inhibited in the four mutants that lack cytoplasmic microtubules, but it is not significantly inhibited in the two mutants that possess cytoplasmic microtubules. In particular, nuclear migration occurs in *tub2-402* mutants even though most of these cells contain exclusively cytoplasmic microtubules. These results indicate that cytoplasmic microtubules, but not nuclear microtubules, are necessary for nuclear migration in yeast.

The fact that the cytoplasmic microtubules are attached to the nuclear envelope at the spindle pole body suggests that these microtubules exert a pulling force on the nucleus to bring it into the bud neck. This model is consistent with the observations that the cytoplasmic microtubules always precede the nucleus into the bud neck and the spindle pole body is situated adjacent to the site of bud emergence (Adams and Pringle, 1984; Byers and Goetsch, 1975; Kilmartin and Adams, 1984). This type of movement would be distinct from the movement of organelles along the surface of microtubules but may involve a mechanism similar to that used to draw chromosomes toward the spindle poles. Although many of the *cdc* mutations block nuclear division (Pringle and Hartwell, 1981), *tub2-104*, *tub2-401*, *tub2-403*, and *tub2-405* are the only *cdc* mutations known to block nuclear migration.

There is evidence that microtubules are involved in nuclear migration in other fungal systems as well. A cold-sensitive mutation in one of the α-tubulin genes of the fission yeast *Schizosaccharomyces pombe* causes aberrant nuclear localization at the nonpermissive temperature (Toda et al., 1983, 1984; Umesono et al., 1983). In *Aspergillus nidulans*, nuclear migration during hyphal growth is inhibited by benomyl and by cold-sensitive mutations in the gene encoding β-tubulin (Oakley and Morris, 1980, 1981).

Cytoplasmic Microtubules Are Essential for Nuclear Migration and Fusion during Conjugation

Nuclear migration and fusion during conjugation are blocked in the four mutants that lack cytoplasmic microtubules, but are permitted to different degrees by the two mutants that possess cytoplasmic microtubules. Significantly, nuclear fusion occurs in *tub2-402* mutants even though most of these cells contain exclusively cytoplasmic microtubules. The results suggest that cytoplasmic microtubules are necessary for nuclear movement during conjugation as well as during mitotic growth. The idea that cytoplasmic microtubules draw nuclei together is consistent with the observations that these microtubules appear to interconnect the spindle pole bodies of the two haploid nuclei, that the movement of nuclei is led by their spindle pole bodies, and that nuclear fusion is initiated at the spindle pole bodies (Byers, 1981; Byers and Goetsch, 1975).

Two criteria were used to assess the effects of the *tub2* mutations on nuclear migration and nuclear fusion during conjugation. A genetic test measured nuclear fusion directly by determining the ploidy of first zygotic buds. This test required that large-budded zygotes formed in the cold be shifted back to permissive temperature to complete nuclear division and cytokinesis. Four of the *tub2* mutations block nuclear fusion indicating that the shift back to permissive temperature did not allow nuclear fusion even though the *tub2* defect is reversed and mitosis proceeds. It appears, then, that nuclear fusion must occur soon after cytoplasmic fusion or it will not occur at all. The results of the genetic test were confirmed by microscopic examination of nuclei in large bud–arrested zygotes. The four mutations that produced a defect in nuclear fusion also prevented the movement of haploid nuclei toward each other. The other two mutations produced zygotes with a single nuclear staining region indicating that nuclear migration and fusion occurred.

Nuclear fusion occurs efficiently in matings between a *tub2-104* or *tub2-401* mutant and a wild-type strain in the

cold. By definition, then, these are "bilateral" karyogamy-defective mutations because both parental strains must be mutant to observe a karyogamy defect. These differ from the "unilateral" *kar1* mutation: a karyogamy defect is observed when only one of the parental strains is *kar1* (Conde and Fink, 1976). It has been shown that the *KAR1* gene product must act before cell fusion (Dutcher and Hartwell, 1983). The bilateral nature of these *tub2* mutations could be explained if microtubule function in the mutant cell is not required before cell fusion. After cell fusion, the wild-type cytoplasm may provide tubulin that can be assembled into microtubules at the mutant cell's spindle pole body. An alternative explanation is that tubulin function in both cells is redundant. It may be sufficient that microtubules originate from only one of the two nuclear envelopes during mating. Our results do not distinguish these possibilities.

Cytoplasmic Microtubules Do Not Play a Role in Secretory Vesicle Transport

Movement of vesicles and organelles along the length of microtubules has been demonstrated in vitro and in vivo (Allen et al., 1982; Vale et al., 1985). The observation that cytoplasmic microtubules extend into the cell bud (Byers, 1981; Byers and Goetsch, 1975; Kilmartin and Adams, 1984) has led to the suggestion that these microtubules are responsible for the transport of secretory vesicles in yeast. However, the *tub2* mutations demonstrate that cytoplasmic microtubules do not play an essential role in the transport of secretory vesicles. None of the *tub2* mutations inhibit bud formation. Even cells carrying the nonfunctional allele, *tub2-401*, arrest as large-budded cells. In addition, invertase secretion is not affected by these mutations. We have not ruled out the possibility that cytoplasmic microtubules play a role in distributing other organelles to the bud before cell division. However, DAPI staining of the large bud-arrested *tub2* mutant cells indicates that all of the buds contain mitochondrial DNA. It, therefore, appears unlikely that mitochondrial transport requires microtubules.

We thank John Kilmartin and Frank Solomon for providing antibodies; John Pringle for communicating results before publication; and Frank Solomon, Alison Adams, and David Drubin for comments on the manuscript.

This work was supported by a postdoctoral fellowship from the Helen Hay Whitney Foundation to Tim C. Huffaker and by grants from National Institutes of Health (GM18973 and GM21253) to David Botstein.

Received for publication 13 November 1987, and in revised form 2 February 1988.

References

Adams, A. E. M., and J. R. Pringle. 1984. Relationship of actin and tubulin distribution to bud growth in wild-type and morphogenetic-mutant *Saccharomyces cerevisiae*. *J. Cell Biol.* 98:934–945.

Allen, R. D., J. Metuzals, I. Tasaki, S. T. Brady, and S. P. Gilbert. 1982. Fast axonal transport in squid giant axon. *Science (Wash. DC).* 218:1127–1128.

Boeke, J. D., F. Lacroute, and G. R. Fink. 1984. A positive selection for mutants lacking orotidine-5'-phosphate decarboxylate activity in yeast: 5-fluoro-orotic acid resistance. *Mol. & Gen. Genet.* 197:345–347.

Bond, J. F., J. L. Fridovich-Keil, L. Pillus, R. C. Mulligan, and F. Solomon. 1986. A chicken-yeast chimeric β-tubulin protein is incorporated into mouse microtubules *in vivo*. *Cell.* 44:461–468.

Byers, B. 1981. Cytology of the yeast life cycle. *In* The Molecular Biology of the Yeast *Saccharomyces*: Life Cycle and Inheritance. J. N. Strathern, E. W. Jones, and J. R. Broach, editors. Cold Spring Harbor Laboratory, Cold Spring Harbor, New York. 59–96.

Byers, B., and L. Goetsch. 1975. Behavior of spindles and spindle plaques in the cell cycle and conjugation of *Saccharomyces cerevisiae*. *J. Bacteriol.* 124:511–523.

Carlson, M., and D. Botstein. 1982. Two differentially regulated mRNAs with different 5' ends encode secreted and intracellular forms of yeast invertase. *Cell.* 28:145–154.

Conde, J., and G. R. Fink. 1976. A mutant of *Saccharomyces cerevisiae* defective for nuclear fusion. *Proc. Natl. Acad. Sci. USA.* 73:3651–3655.

Delgado, M. A., and J. Conde. 1984. Benomyl prevents nuclear fusion in *Saccharomyces cerevisiae*. *Mol. & Gen. Genet.* 193:188–189.

Dustin, P. 1984. Microtubules. 2nd ed. Springer-Verlag New York Inc., New York. 452 pp.

Dutcher, S. K., and L. H. Hartwell. 1983. Genes that act before conjugation to prepare the *Saccharomyces cerevisiae* nucleus for caryogamy. *Cell.* 33: 203–210.

Esposito, R. E., and S. Klapholz. 1981. Meiosis and Ascospore Development. *In* The Molecular Biology of the Yeast *Saccharomyces*; Life Cycle and Inheritance. J. N. Strathern, E. W. Jones, and J. R. Broach, editors. Cold Spring Harbor Laboratory, Cold Spring Harbor, New York. 211–288.

Field, C., and R. Schekman. 1980. Localized secretion of acid phosphatase reflects the pattern of cell surface growth in *Saccharomyces cerevisiae*. *J. Cell Biol.* 86:123–128.

Goldstein, D., and J. Lampen. 1975. Beta-D-fructofuranoside fructohydrolase from yeast. *Methods Enzymol.* 42:504–511.

Hartwell, L. H., and D. Smith. 1985. Altered fidelity of mitotic chromosome transmission in cell cycle mutants of *S. cerevisiae*. *Genetics.* 110:381–395.

Hartwell, L. H., R. K. Mortimer, J. Culotti, and M. Culotti. 1973. Genetic control of the cell division cycle in yeast. V. Genetic analysis of *cdc mutants*. *Genetics.* 74:267–286.

Holm, C., D. W. Meeks-Wagner, W. L. Fangman, and D. Botstein. 1986. A rapid, efficient method for isolating DNA from yeast. *Gene (Amst.).* 42:169–173.

Hutter, K. J., and H. E. Eipel. 1978. Flow cytometric determinations of cellular substances in algae, bacteria, molds and yeasts. *Antonie Leeuwenhoek J. Microbiol. Serol.* 44:269–282.

Kilmartin, J. V. 1981. Purification of yeast tubulin by self-assembly *in vitro*. *Biochemistry.* 20:3629–3633.

Kilmartin, J. V., and A. E. M. Adams. 1984. Structural rearrangements of tubulin and actin during the cell cycle of the yeast *Saccharomyces*. *J. Cell Biol.* 98:922–933.

Kirschner, M., and T. Mitchison. 1986. Beyond self-assembly: from microtubules to morphogenesis. *Cell.* 45:329–342.

Lowry, O. H., N. J. Rosebrough, A. L. Farr, and R. J. Randall. 1951. Protein measurement with Folin phenol reagent. *J. Biol. Chem.* 193:265–275.

McIntosh, J. R. 1982. Mitosis and the cytoskeleton. *In* Developmental Order: Its Origin and Regulation (40th Symposium of the Society for Developmental Biology). Alan R. Liss Inc., New York. 77–115.

McKiethan, T. W., and J. L. Rosenbaum. 1984. The biochemistry of microtubules. *In* Cell and Muscle Motility. Vol. 5. J. W. Shay, editor. Plenum Publishing Corp., New York. 255–288.

Neff, N. F., J. H. Thomas, P. Grisafi, and D. Botstein. 1983. Isolation of the β-tubulin gene from yeast and demonstration of its essential function *in vivo*. *Cell.* 33:211–219.

Novick, P., and R. Schekman. 1979. Secretion and cell-surface growth are blocked in a temperature-sensitive mutant of *Saccharomyces cerevisiae*. *Proc. Natl. Acad. Sci. USA.* 76:1858–1862.

Novick, P., C. Field, and R. Schekman. 1980. Identification of 23 complementation groups required for post-translational events in the yeast secretory pathway. *Cell.* 21:205–215.

Oakley, B. R., and N. R. Morris. 1980. Nuclear movement is β-tubulin-dependent in *Aspergillus nidulans*. *Cell.* 19:255–262.

Oakley, B. R., and N. R. Morris. 1981. A β-tubulin mutation in *Aspergillus nidulans* that blocks microtubule function without blocking assembly. *Cell.* 24:837–845.

Olmsted, J. B. 1986. Microtubule-associated proteins. *Annu. Rev. Cell Biol.* 2:421–457.

Orr-Weaver, T. L., J. W. Szostak, and R. J. Rothstein. 1981. Yeast transformation: a model system for the study of recombination. *Proc. Natl. Acad. Sci. USA.* 78:6354–6358.

Peterson, J. B., and H. Ris. 1976. Electron-microscopic study of the spindle and chromosome movement in the yeast *Saccharomyces cerevisiae*. *J. Cell Sci.* 22:219–242.

Pillus, L., and F. Solomon. 1986. Components of microtubular structures in *Saccharomyces cerevisiae*. *Proc. Natl. Acad. Sci. USA.* 83:2468–2472.

Pringle, J. R., and L. H. Hartwell. 1981. The *Saccharomyces cerevisiae* cell cycle. *In* The Molecular Biology of the Yeast *Saccharomyces*: Life Cycle and Inheritance. J. N. Strathern, E. W. Jones, and J. R. Broach, editors. Cold Spring Harbor Laboratory, Cold Spring Harbor, New York. 97–142.

Pringle, J. R., S. H. Lillie, A. E. M. Adams, C. W. Jacobs, B. K. Haarer, K. G. Coleman, J. S. Robinson, L. Bloom, and R. A. Preston. 1986. Cellular morphogenesis in the yeast cell cycle. *In* Yeast Cell Biology. J. Hicks, editor. Alan R. Liss Inc., New York. 47–80.

Purich, D. L., and D. Kristofferson. 1984. Microtubule assembly: a review of progress, principles and perspectives. *Adv. Protein Chem.* 36:133–212.

Quinlan, R. A., C. I. Pogson, and K. Gull. 1980. The influence of the microtubule inhibitor, methyl benzimidazol-2-yl-carbamate (MBC) on nuclear division and the cell cycle in *Saccharomyces cerevisiae*. *J. Cell Sci.* 46:341–352.

Roberts, K., and J. S. Hyams. 1979. Microtubules. Academic Press Inc., New York. 595 pp.

Robinow, C. F. 1975. The preparation of yeasts for light microscopy. *Methods Cell Biol.* 11:1–22.

Rose, M., and D. Botstein. 1983. Structure and function of the yeast *URA3* gene. *J. Mol. Biol.* 170:883–904.

Rose, M. D., and G. R. Fink. 1987. *KAR1*, a gene required for function of both intranuclear and extranuclear microtubules in yeast. *Cell.* 48:1047–1060.

Sanger, J., S. Nicklen, and A. R. Coulson. 1977. DNA sequencing with chain-terminating inhibitors. *Proc. Natl. Acad. Sci. USA.* 74:5463–5467.

Schatz, P. J., L. Pillus, P. Grisafi, F. Solomon, and D. Botstein. 1986. Two functional α-tubulin genes of the yeast *Saccharomyces cerevisiae* encode divergent proteins. *Mol. Cell. Biol.* 6:3711–3721.

Scherer, S., and R. W. Davis. 1979. Replacement of chromosome segments with altered DNA sequences constructed *in vitro*. *Proc. Natl. Acad. Sci. USA.* 76:4951–4955.

Sherman, F., G. R. Fink, and C. W. Lawrence. 1979. Methods in Yeast Genetics. Cold Spring Harbor Laboratory, Cold Spring Harbor, New York.

Shortle, D., and D. Botstein. 1983. Directed mutagenesis with sodium bisulfite. *Methods Enzymol.* 100:457–468.

Shortle, D., P. Grisafi, S. J. Benkovic, and D. Botstein. 1982. Gap misrepair mutagenesis: efficient site-directed induction of transition, transversion, and frameshift mutations *in vitro*. *Proc. Natl. Acad. Sci. USA.* 79:1588–1592.

Shortle, D., P. Novick, and D. Botstein. 1984. Construction and genetic characterization of temperature-sensitive mutant alleles of the yeast actin gene. *Proc. Natl. Acad. Sci. USA.* 81:4889–4893.

Simchen, G. 1974. Are mitotic functions required in meiosis? *Genetics.* 76: 745–753.

Thomas, J. H., N. F. Neff, and D. Botstein. 1985. Isolation and characterization of mutations in the β-tubulin gene of *Saccharomyces cerevisiae*. *Genetics.* 112:715–734.

Tkacz, J., and J. Lampen. 1972. Wall replication in *Saccharomyces* species: use of fluorescein-conjugated concanavalin A to reveal the site of mannan insertion. *J. Gen. Microbiol.* 72:243–247.

Tkacz, J., and J. Lampen. 1973. Surface distribution of invertase on growing *Saccharomyces cerevisiae*. *J. Bacteriol.* 113:1073–1075.

Toda, T., Y. Adachi, Y. Hiraoka, and M. Yanagida. 1984. Identification of the pleiotropic cell division cycle gene *NDA2* as one of two different α-tubulin genes in *Schizosaccharomyces pombe*. *Cell.* 37:233–242.

Toda, T., K. Umesono, A. Hirata, and M. Yanagida. 1983. Cold-sensitive nuclear division arrest mutants of the fission yeast *Schizosaccharomyces pombe*. *J. Mol. Biol.* 168:251–270.

Umesono, K., T. Toda, S. Hayashi, and M. Yanagida. 1983. Two cell division cycle genes NDA2 and NDA3 of the fission yeast *Schizosaccharomyces pombe* control microtubular organization and sensitivity to anti-mitotic benzimidazole compounds. *J. Mol. Biol.* 168:271–284.

Vale, R. D., B. J. Schnapp, T. S. Reese, and M. P. Sheetz. 1985. Organelle, bead, and microtubule translocations promoted by soluble factors from the squid giant axon. *Cell.* 40:559–569.

Wood, J. S. 1982. Genetic effects of methyl benzimidazole-2-yl carbamate on *Saccharomyces cerevisiae*. *Mol. Cell. Biol.* 2:1064–1079.

Wood, J. S., and L. H. Hartwell. 1982. A dependent pathway of gene functions leading to chromosome segregation in *Saccharomyces cerevisiae*. *J. Cell Biol.* 94:718–726.